Communication

Pyrene-Zipper Array Assembled via RNA Duplex Formation

Mitsunobu Nakamura, Yohei Murakami, Kazuhiro Sasa, Haruhisa Hayashi, and Kazushige Yamana

J. Am. Chem. Soc., **2008**, 130 (22), 6904-6905 • DOI: 10.1021/ja801054t • Publication Date (Web): 13 May 2008

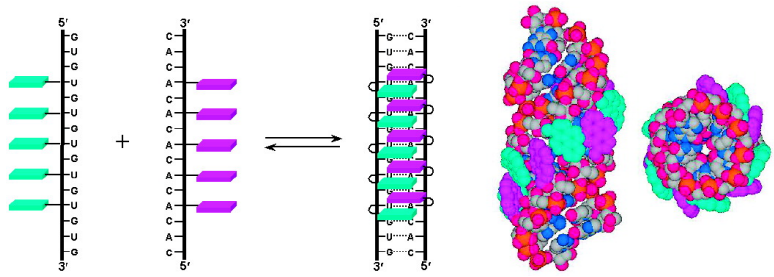

More About This Article

Additional resources and features associated with this article are available within the HTML version:

- Supporting Information
- Links to the 2 articles that cite this article, as of the time of this article download
- Access to high resolution figures
- Links to articles and content related to this article
- Copyright permission to reproduce figures and/or text from this article

View the Full Text HTML

J|A|C|S COMMUNICATIONS

Published on Web 05/13/2008

Pyrene-Zipper Array Assembled via RNA Duplex Formation

Mitsunobu Nakamura,* Yohei Murakami, Kazuhiro Sasa, Haruhisa Hayashi, and Kazushige Yamana*

Department of Materials Science and Chemistry, Graduate School of Engineering, University of Hyogo, 2167 Shosha, Himeji, Hyogo 671-2280, Japan

Received February 11, 2008; E-mail: mitunobu@eng.u-hyogo.ac.jp; yamana@eng.u-hyogo.ac.jp

DNA and RNA can be used as scaffolds in a bottom-up approach to arrange molecules in nanoarchitectures. Among nucleic acid-based nanoobjects, spatially arranged π-aromatic chromophores are currently of interest because they provide an efficient medium for excitation energy and electron migration, which would be usable in functional nanomaterials, such as in photonic devices.[1−10]

In order to develop DNA/RNA-based devices, as well as to develop fluorescent nucleic acid probes, we focused on RNA oligomers having multipyrenylmethyl groups at the 2′-*O*-sugar residues. We found that pyrene-modified RNAs such as 5′-$(U_{OME})_8X_4(U_{OME})_7U$, **P4** (where U_{OME} is 2′-*O*-methyluridine and X is 2′-*O*-pyrenylmethyluridine), can bind to rA_{20} to yield A-form duplexes without loss of thermal stability. Crucially, the pyrenes are helically assembled along the outside of duplex RNA that exhibits strong excimer fluorescence.[11]

We describe here a new type of multipyrene-modified RNA sequence that can be used to produce a specific structure of a pyrene aromatic array on an RNA duplex that can emit remarkably strong excimer fluorescence.

The sequences of the pyrene-modified RNAs are shown in Chart 1. One RNA sequence (**X5**) contains five pyrene-modified uridines (U_{Py}), two of which are separated by an intervening ribonucleoside. The other strand (**Y5**) has pyrene-adenosine (A_{Py}) in the same way as **X5**, and its sequence is complementary to the U_{py}-containing strand. With this design, during interstrand association between **X5** and **Y5**, interactions between pyrenes will form an aromatic array on the duplex. The process of pyrene array formation differs from that of the first version (**P4-rA$_{20}$**) and somewhat resembles zipper formation. We therefore call this particular arrangement a "pyrene-zipper array" (Figure 1).[12]

Table 1 summarizes the melting temperatures (T_m), the peak-to-valley intensity ratios (P_A) in the absorptions, and the ratios of intensities of excimer and monomer fluorescence (I_E/I_M) of the RNA duplexes. The T_m values for **X*n*−Y0** and **X0−Y*n*** (n = 1 or 5) containing pyrenes in one strand were lower than that for unmodified duplex **X0−Y0**. Significantly, the T_m values for **X5−Y5** having pyrenes in both strands were higher than those for **X*n*−Y0** and **X0−Y*n***, and they were very close to those for **X1−Y1** and **X0−Y0**. These binding experiments thus suggest that the interstrand pyrene association occurs in the ground state for **X1−Y1** and **X5−Y5**.

The interstrand interactions between pyrenes during the formation of RNA duplexes (**X1−Y1** and **X5−Y5**) were determined from the absorption and fluorescence spectra shown in Figure 2. The duplex **X1−Y1** exhibited absorption bands at 336 and 351 nm that were 1−2 nm longer than those of **X1** and **Y1**. In the fluorescence spectrum of **X1−Y1**, pyrene excimer fluorescence was observed at 487 nm with an I_E/I_M value of 0.38, whereas **X1−Y0** and **X0−Y1** duplexes did not exhibit any excimer fluorescence. Therefore, these spectroscopic observations strongly suggest that the two pyrenes located at the outside of the duplex are able to interact with each other, producing the characteristic emission. In a manner similar to that of the two-pyrene-

Chart 1. Sequences of Pyrene-Modified RNAs

X0: 5′-rGUG UGU GUG UGU GUG-3′
X1: 5′-rGUG UGU G**U$_{Py}$**G UGU GUG-3′
X5: 5′-rGUG **U$_{Py}$GU$_{Py}$** G**U$_{Py}$**G **U$_{Py}$GU$_{Py}$** GUG-3′

Y0: 5′-rCAC ACA CAC ACA CAC-3′
Y1: 5′-rCAC ACA C**A$_{Py}$**C ACA CAC-3′
Y5: 5′-rCAC **A$_{Py}$CA$_{Py}$** C**A$_{Py}$**C **A$_{Py}$CA$_{Py}$** CAC-3′

U_{Py} = 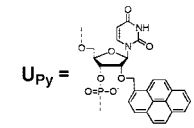

A_{Py} = 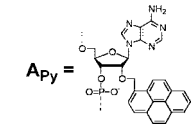

modified duplex (**X1−Y1**), the pyrene absorption bands of **X5−Y5** appeared at 336 and 351 nm, which are slightly longer than those of **X5** and **Y5**. Crucially, the absorption intensity at 336 nm was stronger than that at 351 nm, yielding a P_A value of 1.1, which is relatively low compared to those of the other duplexes (**X1−Y1** = 1.3, **X5−Y0** = 1.5, and **X0−Y5** = 1.5).[13] The fluorescence spectrum of **X5−Y5** exhibited extremely strong excimer fluorescence at 490 nm (φ = 0.22),

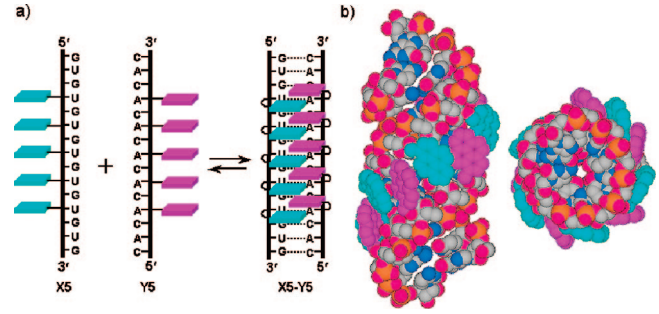

Figure 1. Schematic representation (a) of duplex formation between multipyrene-modified RNA sequences (**X5−Y5**). Side view and top view (b) of duplex structure of **X5−Y5**. The pyrenes of **X5** are cyan and the pyrenes of **Y5** are magenta.

Table 1. Melting Temperatures (T_m), Peak-to-Valley Intensity Ratios (P_A), and Ratios of Intensities of Excimer and Monomer Fluorescence (I_E/I_M) of RNA Duplexes

duplex	T_m/°C[a]	P_A[b]	I_E/I_M[c]
X0−Y0	68		
X1−Y0	65	1.3	
X0−Y1	62	1.6	
X1−Y1	65	1.3	0.38
X5−Y0	47	1.5	0.11
X0−Y5	37	1.5	0.46
X5−Y5	68	1.1	6.7

[a] T_m was obtained from the first derivatives of the transition profiles monitored by absorption changes at 260 nm in a buffer of pH 7 containing 0.1 M NaCl, 0.01 M $NaHPO_4$, and 1 mM EDTA. [b] P_A was calculated from the absorption intensity of the red edge band and that of the adjacent minimum at shorter wavelengths. [c] I_E/I_M was calculated from the fluorescence intensity of the monomer (378 nm) and excimer (490 nm).

10.1021/ja801054t CCC: $40.75

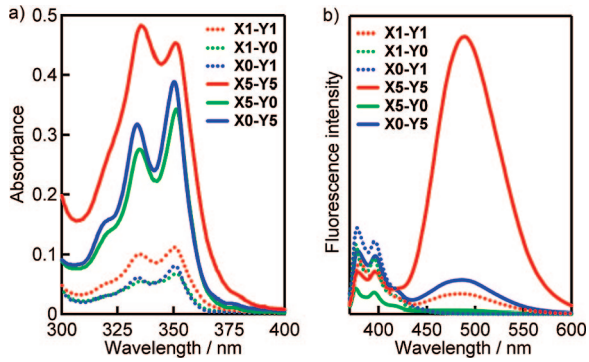

Figure 2. Absorption (a) and fluorescence (b) spectra of the RNA duplexes (3.3 μM) in a buffer of pH 7 containing 0.1 M NaCl, 0.01 M $NaHPO_4$, and 1 mM EDTA. Fluorescence spectra were measured with excitation at 350 nm.

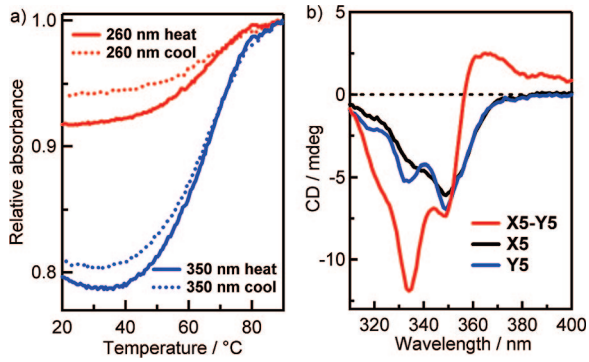

Figure 3. Melting and reverse-melting profiles (a) and CD spectrum (b) of **X5**−**Y5** (3.3 μM) in a buffer of pH 7 containing 0.1 M NaCl, 0.01 M $NaHPO_4$, and 1 mM EDTA. The CD spectra of single-stranded **X5** and **Y5** are shown for comparison.

with a high I_E/I_M value of 6.7. The intensity of the excimer fluorescence of **X5**−**Y5** was almost 10 times greater than that of **X1**−**Y1**. In contrast, **X5**−**Y0** and **X0**−**Y5** duplexes exhibited weak excimer fluorescence, with I_E/I_M values lower than 0.5. These observations strongly suggest that the ground-state interactions of pyrenes in the duplexes (**X5**−**Y5**) are significant relative to those of the single-strand oligomers (**X5** and **Y5**) and to those of the two-pyrene-modified duplex (**X1**−**Y1**).

Figure 3a shows the thermal dissociation and association profiles for a 1:1 mixture of **X5** and **Y5** (total strand concentration = 3.3 μM) obtained by temperature-dependent UV−visible spectra. The duplex melting curves, both at 260 and 350 nm, displayed single-phase transitions having shapes that are relatively broad but resemble that of the unmodified RNA duplex (**X0**−**Y0**). From the thermal melting and thermal back profiles, the dissociation and association of **X5**−**Y5** proceeded with only slight hysteresis. The hyperchromic change observed at the pyrene absorption (350 nm) during the duplex melting indicates that the interactions between pyrenes occurred in a cooperative manner with the formation of the RNA duplex.

Figure 3b shows the CD spectrum of **X5**−**Y5** in the range of the pyrene absorption. The CD spectra of single-stranded **X5** and **Y5** are also given for comparison. The duplex **X5**−**Y5** exhibited a positive Cotton effect in the ^1L_a transition of pyrene, whereas no such positive Cotton effect was observed for single-stranded **X5** and **Y5**. The single-stranded pyrene-modified RNAs exhibited only negative-induced CD signals in this region. The observed induced CD of **X5**−**Y5** is consistent with an arrangement of pyrenes along the minor groove of a duplex RNA. A positive Cotton effect in the CD at the pyrene absorption region has been observed for the four-pyrene-modified RNA duplexes (**P4-rA$_{20}$**).[11]

In summary, our strategy of pyrene modification of RNA is useful for constructing a pyrene-zipper array in which formation is controllable by RNA hybridization. These results provide important insights for the development of RNA architectures that conduct excitation energy and charges.

Acknowledgment. The authors thank Profs. Takashi Sugimura and Morifumi Fujita for the measurements of CD spectra. This research was supported by a Grant-in-Aid for Scientific Research from the Japan Society for the Promotion of Science (JSPS).

Supporting Information Available: Experimental details. This material is available free of charge via the Internet at http://pubs.acs.org.

References

(1) For pyrene-modified DNA/RNA, see: (a) Wilson, J. N.; Teo, Y. N.; Kool, E. T. *J. Am. Chem. Soc.* **2007**, *129*, 15426–15427. (b) Cho, Y.; Kool, E. T. *ChemBioChem* **2006**, *7*, 669–672. (c) Mayer-Enthart, E.; Wagenknecht, H.-A. *Angew. Chem., Int. Ed.* **2006**, *45*, 3372–3375. (d) Barbaric, J.; Wagenknecht, H.-A. *Org. Biomol. Chem* **2006**, *4*, 2088–2090. (e) Malinovskii, V. L.; Samain, F.; Häner, R. *Angew. Chem., Int. Ed.* **2007**, *46*, 4464–4467. (f) Langenegger, S. M.; Häner, R. *Chem. Commun.* **2004**, 2792–2793. (g) Hrdicka, P.; Babu, B. R.; Sørensen, M. D.; Harrit, N.; Wengel, J. *J. Am. Chem. Soc.* **2005**, *127*, 13293–13299.

(2) For perylene-modified DNA, see: (a) Wang, W.; Wan; W.; Zhou, H.-H.; Niu, S.; Li, A. D. Q. *J. Am. Chem. Soc.* **2003**, *125*, 5248–5249. (b) Wang, W.; Li, A. D. Q. *Bioconjugate Chem.* **2007**, *18*, 1036–1052.

(3) For fluorescein-modified DNA, see: Gierlich, J.; Burley, G. A.; Gramlich, P. M. E.; Hammond, D. M.; Carell, T. *Org. Lett.* **2006**, *8*, 3639–3642.

(4) For stilbene-modified DNA, see: (a) Lewis, F. D.; Zhang, L.; Zuo, X. *J. Am. Chem. Soc.* **2005**, *127*, 10002–10003. (b) Lewis, F. D.; Zhang, L.; Liu, X.; Zuo, X.; Tiede, D. M.; Long, H.; Schatz, G. C. *J. Am. Chem. Soc.* **2005**, *127*, 14445–14453.

(5) For methyl-red-modified DNA, see: (a) Asanuma, H.; Shirakusa, K.; Takarada, T.; Kashida, H.; Komiyama, M. *J. Am. Chem. Soc.* **2003**, *125*, 2217–2223. (b) Asanuma, H.; Liang, X.; Nishioka, H.; Matsunaga, D.; Liu, M.; Komiyama, M. *Nat. Protoc.* **2007**, *2*, 203–212.

(6) For porphyrin-modified DNA, see: Fendt, L. A.; Bouamaied, I.; Thöni, S.; Amiot, N.; Stulz, E. *J. Am. Chem. Soc.* **2007**, *129*, 15319–15329.

(7) For metal−ligand complexations in DNA, see: (a) Tanaka, K.; Tengeiji, A.; Kato, T.; Toyama, N.; Shionoya, M. *Science* **2003**, *299*, 1212–1213. (b) Tanaka, K.; Clever, G. H.; Takezawa, Y.; Yamada, Y.; Kaul, C.; Shionoya, M.; Carell, T. *Nat. Nanotechnol.* **2006**, *1*, 190–194.

(8) For biphenyl-modified DNA, see: (a) Brotschi, C.; Mathis, G.; Leumann, C. J. *Chem.—Eur. J.* **2005**, *11*, 1911–1923. (b) Stoop, M.; Zahn, A.; Leumann, C. J. *Tetrahedron* **2006**, *63*, 3440–3449.

(9) For noncovalent chromophore aggregation on DNA, see: (a) Janssen, P. G. A.; Vandenbergh, J.; van Dongen, J. L. J.; Meijer, E. W.; Schenning, A. P. H. J. *J. Am. Chem. Soc.* **2007**, *129*, 6078–6079. (b) Dilek, I.; Madrid, M.; Singh, R.; Urrea, C. P.; Armitage, B. A. *J. Am. Chem. Soc.* **2005**, *127*, 3339–3345. (c) Hannah, K. C.; Armitage, B. A. *Acc. Chem. Res.* **2004**, *37*, 845–853.

(10) For photonic wire using DNA, see: (a) Sanchez-Mosteiro, G.; van Dijk, E. M. H. P.; Hernando, J.; Heilemann, M.; Tinnefeld, P.; Sauer, M.; Koberlin, F.; Patting, M.; Wahl, M.; Erdmann, R.; van Hulst, N. F.; Garcia-Parajo, M. F. *J. Phys. Chem. B* **2006**, *110*, 26349–26353. (b) Heilemann, M.; Kasper, R.; Tinnefeld, P.; Sauer, M. *J. Am. Chem. Soc.* **2006**, *128*, 16864–16875.

(11) (a) Nakamura, M.; Ohtoshi, Y.; Yamana, K. *Chem. Commun.* **2005**, 5163–5165. (b) Nakamura, M.; Shimomura, Y.; Ohtoshi, Y.; Sasa, K.; Hayashi, H.; Nakano, H.; Yamana, K. *Org. Biomol. Chem.* **2007**, *5*, 1945–1951.

(12) The energy minimized structure in Figure 1b was constructed according to the method described in: Nakamura, M.; Fukunaga, Y.; Sasa, K.; Ohtoshi, Y.; Kanaori, K.; Hayashi, H.; Nakano, H.; Yamana, K. *Nucleic Acids Res.* **2005**, *33*, 5887–5895.

(13) P_A is a good indicator for the extent of the pyrene association. Winnik, F. M. *Chem. Rev.* **1993**, *93*, 587–614. The absorption intensity of **X5**−**Y5** at 351 nm was smaller than the sum of the absorbance of **X5**−**Y0** and **X0**−**Y5**, indicating that the ground-state association of pyrenes in **X5**−**Y5** caused hypochromic effect on the absorption. Similar hypochromicity in the pyrene absorption was observed for **X1**−**Y1**.

JA801054T